

## Article

# Effects of Coloration of Spinel $\text{CoAl}_2\text{O}_4$ Cobalt Blue Pigments: Composition, Structure, and Cation Distribution

Weiran Zhang <sup>1,2</sup> , Ziyu Li <sup>1,2</sup>, Guohua Wu <sup>1,2</sup>, Wei Wu <sup>1</sup>, Hailan Zeng <sup>1</sup>, Haiyun Jiang <sup>1,2,\*</sup> , Weili Zhang <sup>1</sup>, Ruomei Wu <sup>1</sup> and Qiong Xue <sup>1</sup>

<sup>1</sup> School of Packaging and Materials Engineering, Hunan University of Technology, Zhuzhou 412007, China; jetwalkerz@gmail.com (W.Z.); ziyv.lee@gmail.com (Z.L.); wghaiyyr1120@163.com (G.W.); waqarrd@163.com (W.W.); zenghl0424@163.com (H.Z.); zh\_weili@163.com (W.Z.); cailiaodian2004@126.com (R.W.); xueqiong2005@163.com (Q.X.)

<sup>2</sup> National & Local Joint Engineering Research Center for Advanced Packaging Material and Technology, Hunan University of Technology, Zhuzhou 412007, China

\* Correspondence: jhyun@163.com

**Abstract:** Cobalt blue ceramic pigments mainly consisting of  $\text{CoAl}_2\text{O}_4$  are subject to the difficulty of color control. Here, a perspective is reported regarding research on the reasons for color change based on the control of the heat treatment and ratio of components. Macroscopically, the composition of pigment powders determines the color. Microscopically, the crystallite characters including size, cation distribution, and structure have an important effect on the color. The ingredient, structural, and color properties of the pigment powders are analyzed using thermo gravimetry–differential scanning calorimetry (TG–DSC), X-ray diffraction (XRD) measurement, Rietveld refinement, energy dispersive spectrometer (EDS), and colorimetry analysis. The color is proven to be associated with cation distribution, such as that of  $\text{Co}^{2+}$  and  $\text{Co}^{3+}$ . It is indicated that high heating temperature, long heating time, and a large proportion of  $\text{Al}^{3+}$  can, respectively, induce the  $\text{Co}^{2+}$  and  $\text{Al}^{3+}$  in tetrahedral and octahedral sites.

**Keywords:** cobalt blue; ceramics pigment;  $\text{CoAl}_2\text{O}_4$ ; cation distribution; coloration



**Citation:** Zhang, W.; Li, Z.; Wu, G.; Wu, W.; Zeng, H.; Jiang, H.; Zhang, W.; Wu, R.; Xue, Q. Effects of Coloration of Spinel  $\text{CoAl}_2\text{O}_4$  Cobalt Blue Pigments: Composition, Structure, and Cation Distribution. *Inorganics* **2023**, *11*, 368. <https://doi.org/10.3390/inorganics11090368>

Received: 5 August 2023

Revised: 6 September 2023

Accepted: 8 September 2023

Published: 14 September 2023



**Copyright:** © 2023 by the authors. Licensee MDPI, Basel, Switzerland. This article is an open access article distributed under the terms and conditions of the Creative Commons Attribution (CC BY) license (<https://creativecommons.org/licenses/by/4.0/>).

## 1. Introduction

Spinel, a class of cubic crystal structure, is widely researched and applied in many fields related to thermal and chemical stability [1–3] such as catalysts [4,5], pigments [6,7], and refractories. The general formula of spinel could be described as  $\text{AB}_2\text{O}_4$  (shown in Figure 1), in which ions A and B occupy the tetrahedral and octahedral fully or partly [8,9]. Ions A and B are usually divalent, trivalent, or quadrivalent transitional cations, including zinc, magnesium, titanium, iron, chromium, cobalt, and aluminum, etc.

$\text{CoAl}_2\text{O}_4$  powders acting as the main composition of cobalt blue ceramic pigments are widely used in the ceramics industry [1,10–14]. Cobalt blue pigment is an excellent choice for use in underglaze ceramic products because it possesses high stability in coloration and phase at a high temperature, even above 1360 °C [15]. Thus, it can be utilized in underglazed ceramic products, which should have physicochemical and colorimetry stability under a high temperature, over 1300 °C. In recent years, many preparations of  $\text{CoAl}_2\text{O}_4$  have been introduced, including the co-precipitation method [16–18], solution combustion [19,20], grinding and calcining method, molten salt decomposition method, sol–gel method [21], hydrothermal method [22], etc. Among these methods, co-precipitation and sol–gel methods prove helpful for a tiny crystallite size, high purity, and few side reactions.

Pigments mainly composed of  $\text{CoAl}_2\text{O}_4$  are reported to exhibit different colors, not only sky-blue or Thenard’s blue. From the research of Gaudon et al., the pigments present blue and cyan colors after doping  $\text{Zn}^{2+}$  and  $\text{Ni}^{2+}$  in the spinel structure [23]. Even the  $\text{CoAl}_2\text{O}_4$  can show the color change from a pink to pale violet color when certain numbers

of  $\text{Co}^{2+}$  substitute the  $\text{Al}^{3+}$  in octahedral sites and the crystallite size is little enough [24]. Apart from the key reason, cation distribution and coloration also change with the crystallite scale from 0.1 to 10 nm [25,26].

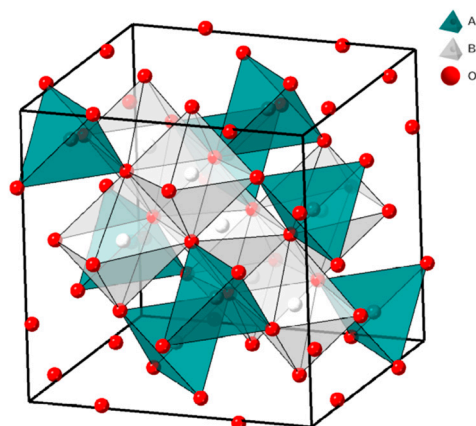


**Figure 1.** The crystal structure of  $\text{AB}_2\text{O}_4$ .

With the large scale and sophisticated development of the ceramics industry, pigments with a high stability, fine particle size, and an easily controlled color have lots of advantages, but nowadays many factories are suffering from the color inconsistency of different batches of pigments. The main shortcoming of the current  $\text{CoAl}_2\text{O}_4$  pigments is that the coloration [27], including hue and saturation, is hard to control; even the discipline of color based on the crystal structures is indistinct. If this problem is solved effectively, not only color accuracy will be improved, but also the cost of raw materials and thermal treatment [11,13,28–30] during aluminum over-stoichiometric spinel synthesis can be cut down.

The reason for color differences consists of two main parts. On the macro-level, related impurities from side reactions are generated during the preparation process. The impurities are associated with the selection of raw materials, the temperature of heat-treatment, pH value, etc. On the micro-level, the free  $\text{Co}^{2+}$  and  $\text{Al}^{3+}$  cannot stay in the tetrahedral and octahedral sites fully and respectively. In addition,  $\text{Co}^{2+}$  can transform into  $\text{Co}^{3+}$  and then occupy both the tetrahedral and octahedral sites partly, which will cause changes in the crystal structure including lattice parameter, bond length, ion radii, etc.

In this paper,  $\text{CoAl}_2\text{O}_4$  powders are elaborated by the co-precipitation method and sintered under different temperatures (250, 500, 800, 1200, 1400 °C). The macroscopical and microscopical factors are deeply discussed including composition, cation distribution, and cation transfer trend related to the increasing ratio and heating temperatures and time. Based on these, the color effects and changing trends corresponding to the ratio and heating condition are obviously reported. These can be a color prediction of the high-temperature  $\text{CoAl}_2\text{O}_4$  pigments and a reference for the doped, cobalt blue pigments through controlling the preparation condition during the fabrication process.

## 2. Results and Discussion

### 2.1. Crystal Phases after Heat Treatment at Different Temperatures

The precursors of cobalt blue pigments are analyzed to figure out the thermal influences on pigments using TG–DSC, which can describe the thermodynamic changes during the heat treatment. Figure 2 demonstrates the TG–DSC curve of the precursor sample sintered in an air atmosphere. Two ranges of room temperature—240 °C and 310–430 °C present obvious weight loss, which could represent the loss of free and bound water, respectively [31]. At the same ranges, the DSC curve does not show any endothermic peaks. In the range from 240 to 310 °C, the stair of weight loss indicates the transformation of precursors to the crystal phase [32]. From the relative DSC curve, a specific exothermic peak occurs at 282 °C, probably related to the burning of ethanol [33]. The weight loss in

the TG curve turns to be stable when the temperature is above 480 °C, which also indicates the gradually stable phase and the formation of a solid solution with cobalt and aluminum ions. The reaction rate declines as the temperature increases, and the exothermal maximum in the DSC curve occurs at 943 °C, while the reaction does not stop completely. Combined with the TG results, it demonstrates that the sample transforms from amorphous phases to relatively stable phases gradually [34]. The loss of weight during the heat-treatment is 20.75%, and the low weight loss (2.82%) in the range of 1000–1400 °C reveals the high thermal stability of the underglaze pigments.

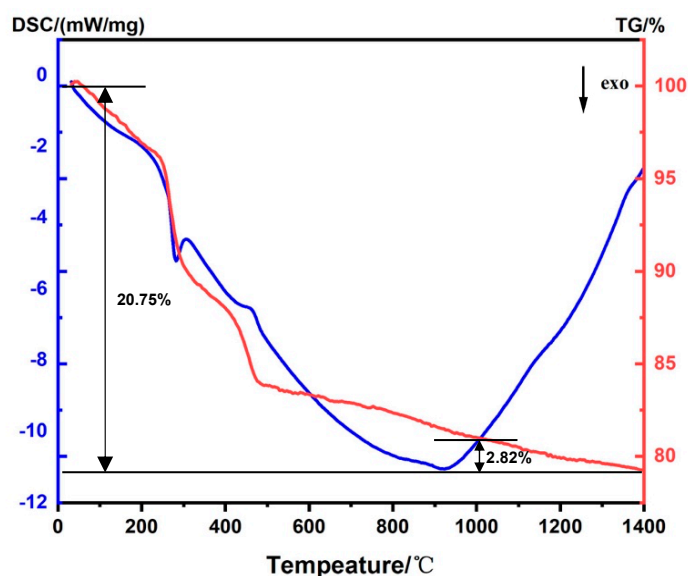


**Figure 2.** TG–DSC curves of precursor (air atmosphere).

The XRD spectra of cobalt blue pigment powders after the heat treatment at different temperatures are presented in Figure 3. According to JCPDS-ICDD cards [35], the as-fabricated  $\text{CoAl}_2\text{O}_4$  powders are composed with a relatively pure spinel structure (*Fd-3m* space group) at 1400 °C. Obviously, the higher the temperature the powders sinter at, the sharper the peaks it will present in the patterns, which means the formation of purer spinel structural phases and a larger particle scale. The peaks on the XRD pattern of the material heat-treated at 250 °C indicate the beginning of the transformation to the spinel structure. In the temperature range of 800–1200 °C, substantial spinel phases form but the phase transformation is not obvious, corresponding with the decrease in the reaction rate seen in the DSC curve (Figure 2).

As represented in Figure 4, the EDS spectrum also confirms the composition of the as-prepared powders at 1400 °C. The EDS spectrum and elemental composition (Table 1) present the composition and the ratio of the pigment powders, agreeing with the XRD results. The ratio of Co and Al still remains as about 1:2, which is in accordance with the experimental design. According to JCPDS-ICDD cards [35,36], the peaks (220), (311), (400), (331), (422), (511), and (440) mainly correspond to a cubic spinel structure. Beginning from 1200 °C, the peak (331) occurs and becomes distinct at 1400 °C, which reveals the formation of the main phase,  $\text{CoAl}_2\text{O}_4$ . The powders heated at 250 °C, 500 °C, and 800 °C are mainly with a spinel phase, with ions occupying the tetrahedral and octahedral positions. However, it seems to be hard to determine the specific phase for diverse cation types. As the heat temperature rises, the main phase transfers to a concrete phase,  $\text{CoAl}_2\text{O}_4$ , gradually. The ratio of the second strongest to the strongest peak is introduced to distinguish two possible phases,  $\text{Co}_3\text{O}_4$  and  $\text{Co}_2\text{AlO}_4$ , because they have similar XRD spectra, and the same Miller index but different intensities [36]. The former  $I(220)/I(311)$  is 0.7 and the latter one is 0.309. Different phases after heat treatment at different temperatures make the pigment powders present different colors. Essentially, the hue is influenced by the cation distribution of

$\text{Co}^{2+}$  and  $\text{Co}^{3+}$  in the spinel framework with a  $Fd-3m$  space group. Both the existence of  $\text{Co}_3\text{O}_4$  (one  $\text{Co}^{2+}$  ion in the tetrahedral site and two  $\text{Co}^{3+}$  ions in the octahedral site) and  $\text{Co}_2\text{AlO}_4$  (one  $\text{Co}^{2+}$  ion in tetrahedral site and one  $\text{Co}^{3+}$  ions in octahedral site) can affect the purity and coloration of cobalt blue pigments.  $\text{Co}_3\text{O}_4$  and  $\text{Co}_2\text{AlO}_4$  will make the color of pigments darker and greener, respectively. The XRD spectra show that the fabrication temperature of pure  $\text{CoAl}_2\text{O}_4$  pigment powders should be 1200 °C or more. Because of the low diffusion rate, many  $\text{Co}^{2+}$  and  $\text{Co}^{3+}$  ions are in tetrahedral and octahedral positions, respectively, at temperatures below 1200 °C, opposite to the ideal phase structure.

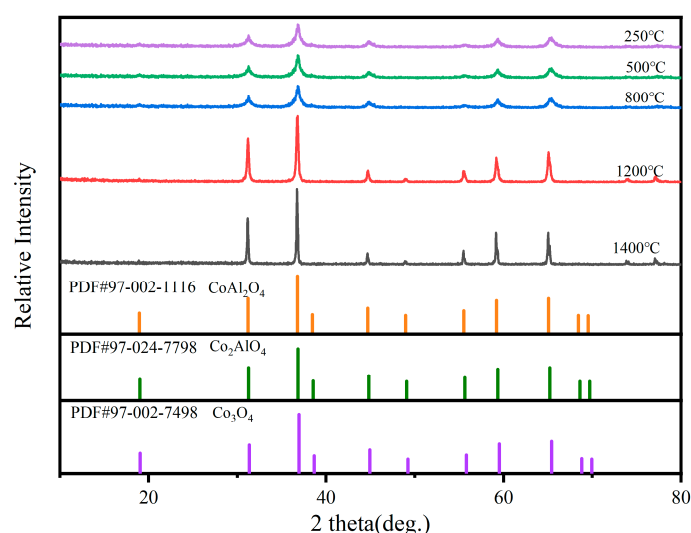


**Figure 3.** XRD patterns of cobalt blue pigments dried via the supercritical method and heated at 1400 °C, 1200 °C, 800 °C, 500 °C, and 250 °C.

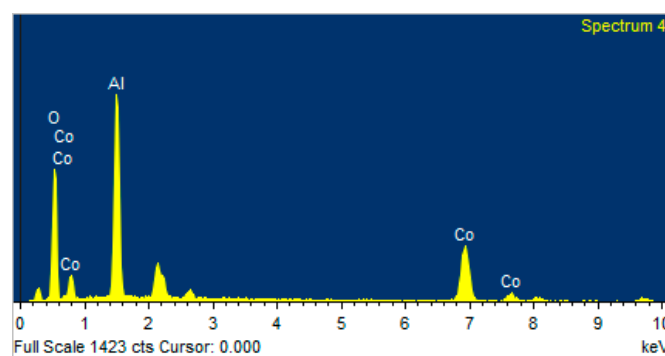


**Figure 4.** EDS spectrum of the  $\text{CoAl}_2\text{O}_4$  sample heating at 1400 °C.

**Table 1.** Composition parameters of the  $\text{CoAl}_2\text{O}_4$  sample heated at 1400 °C.

Element	Weight%	Atomic%
O K	37.46	58.05
Al K	31.39	28.85
Co K	31.15	13.10
Totals	100.00	

## 2.2. Influence Factors of Structural Properties

Composite pigments primarily consist of transition metals from the d-block of the periodic table and the molecules or ions (ligands) that bind to these metals. The fundamental source of its color is the absorption of visible light to produce d–d electronic transitions. The coloration of  $\text{CoAl}_2\text{O}_4$  is mainly determined by the central ions in the tetrahedral and

octahedral coordination fields. Concerning the  $\text{CoAl}_2\text{O}_4$  spinel, they are  $\text{Co}^{2+}$  and  $\text{Al}^{3+}$ , but  $\text{Al}^{3+}$  is colorless because of the completely empty d electron shell. The main reason for the coloration of  $\text{CoAl}_2\text{O}_4$  is  $\text{Co}^{2+}$ .

The appearance of peaks (331) reveals the formation of  $\text{CoAl}_2\text{O}_4$ , and the purity of  $\text{CoAl}_2\text{O}_4$  rises as the sintering temperature increases. Thus, the main reason for the coloration is related to the crystallite structure.

### 2.2.1. Crystallite Size

Table 2 presents the crystallite size,  $X_s$ , of the pigment powders of different batches. The error of the size estimation is 6%. Over 1200 °C, the crystallite size grows with the temperature and time increasing. As is known from previous research, the crystallite size of pigments can affect the optical performance if the scale is between 0.1 and 10 nm [25,26]. From the analysis data, the scale of the crystallite is not enough to influence the coloration.

**Table 2.** Crystallite size of  $\text{CoAl}_2\text{O}_4$  pigment powders after heat treatment at different temperatures and times.

Sample	Temperature (°C)	Time (h)	$X_s$ (Å)
1	1200	1	553
2	1200	1	596
1	1200	3	580
1	1400	1	624
2	1400	1	721

### 2.2.2. Cation Distribution

The formation of a cobalt blue pigment spinel structure for the  $(\text{Co}_x\text{Al}_{1-x})[\text{Al}_{1+x}\text{Co}_{1-x}]\text{O}_4$  ( $0 \leq x \leq 1$ ) system was confirmed by XRD patterns in Figure 5. The fitting profiles and R-factor of the samples are shown as an example in Figure 6. The result is obtained from Retveld refinement using the program Jade. The cation distribution data, including cation position and lattice parameter, are shown in Table 3. Other structural parameters are included in Table 4 for reference. The ratio of cobalt and aluminum is 1:2 in the sample, and the prescription of Sample 2 contains excessive aluminum.

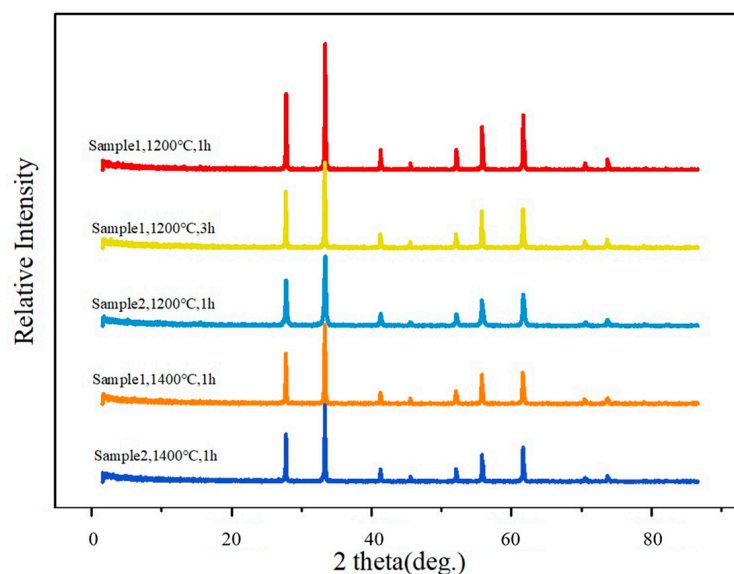


**Figure 5.** XRD patterns of samples in different conditions. Sample 1 is fabricated by the ratio of Co and Al equal to 1:2; sample 2 is fabricated by excessive Al.

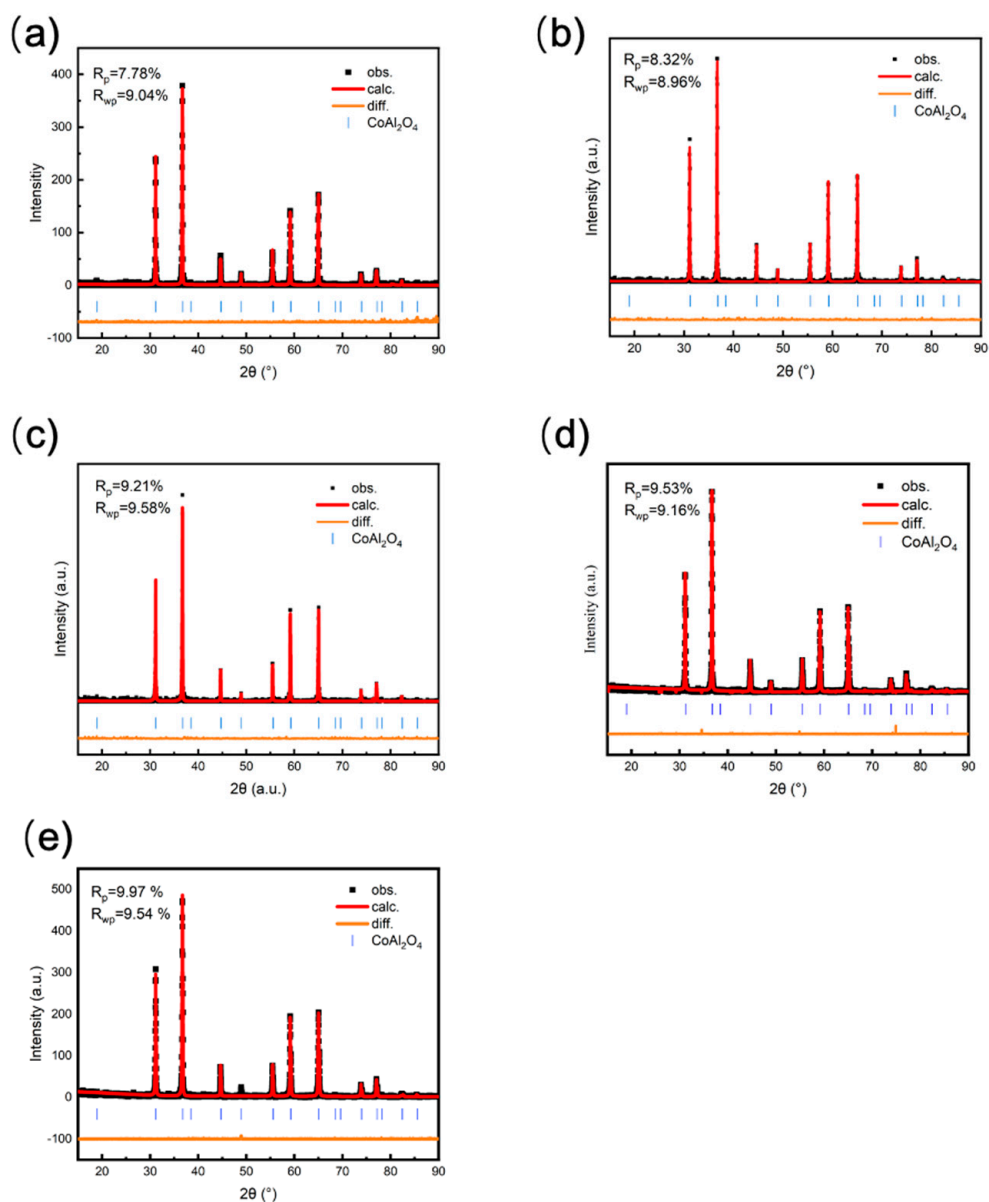


**Figure 6.** Rietveld analysis results of (a) sample 1 after 1200 °C heat treatment for 1 h, (b) sample 2 after 1200 °C heat treatment for 1 h, (c) sample 1 after 1200 °C heat treatment for 3 h, (d) sample 1 after 1400 °C heat treatment for 1 h, and (e) sample 2 after 1400 °C heat treatment for 1 h, including fitting pattern, residual curve, Bragg reflection position, and R-factor.

For the normal ratio part, a high heating temperature and long heating time are both related to the increase in the lattice parameter. Compared with the normal ratio samples, the amount of  $\text{Co}^{3+}$  transferring from the octahedral site to the tetrahedral site enlarges in the crystallite of sample 2. At the same time, the  $\text{Co}^{3+}$  converts into divalent Co, but the quantity of  $\text{Co}^{3+}$  in octahedral sites grows correspondingly. Compared with the sample heated at 1400 °C, the stoichiometric ratio, cation position, and lattice parameter of sample 1 at 1200 °C are all close to those of  $\text{Co}_2\text{AlO}_4$  because the  $\text{Co}_2\text{AlO}_4$  (described as  $(\text{Co})[\text{CoAl}]\text{O}_4$ ) has one  $\text{Co}^{2+}$  in the tetrahedral site and one  $\text{Co}^{3+}$  and one  $\text{Al}^{3+}$  in the octahedral site, with a smaller lattice parameter than  $\text{CoAl}_2\text{O}_4$ . Moreover, whether the heating time or temperature increases, the main phase can change into  $\text{CoAl}_2\text{O}_4$  in line with cation distribution. The result confirms the analysis of Figure 3 which indicates the formation of  $\text{CoAl}_2\text{O}_4$  for the first time at 1200 °C, becoming purer and purer as the temperature rises. Focusing on the cation distribution of sample 1 heated at 1200 °C for 3 h

and 1400 °C for 1 h, the data demonstrate the similar phase and structural properties of them. Moreover, the increase in the aluminum ratio can also promote the occupation of  $\text{Co}^{2+}$  in the tetrahedral site and  $\text{Al}^{3+}$  in the octahedral site. Throughout the increases in the heating time, temperature, and Al element ratio, they all enhance the  $\text{Al}^{3+}$  substitution into the  $\text{Co}^{3+}$  octahedral site, and “push” a part of the Co ions into tetrahedral sites, with the preference of “pushing” the  $\text{Co}^{3+}$  toward the octahedral.

**Table 3.** Cation distribution data calculated from the Rietveld refinement of  $(\text{Co}_x\text{Al}_{1-x})[\text{Al}_{1+x}\text{Co}_{1-x}]\text{O}_4$  ( $0 \leq x \leq 1$ ) system after heat treatment at different temperatures and times.

Sample	Temperature (°C)	Time (h)	Chemical Formula	Occupation of Cations		Lattice Parameter
				Tetrahedral Site	Octahedral Site	
1	1200	1	$\text{Co}_{1.91}\text{Al}_{1.09}\text{O}_4$	$(\text{Co}_{0.75}^{2+}\text{Al}_{0.25}^{3+})$	$[\text{Co}_{0.25}^{2+}\text{Co}_{0.91}^{3+}\text{Al}_{0.84}^{3+}]$	8.096
2	1200	1	$\text{Co}_{1.46}\text{Al}_{1.54}\text{O}_4$	$(\text{Co}_{0.85}^{2+}\text{Al}_{0.15}^{3+})$	$[\text{Co}_{0.46}^{2+}\text{Co}_{0.15}^{3+}\text{Al}_{1.39}^{3+}]$	8.104
1	1200	3	$\text{Co}_{1.39}\text{Al}_{1.61}\text{O}_4$	$(\text{Co}_{0.90}^{2+}\text{Al}_{0.10}^{3+})$	$[\text{Co}_{0.39}^{2+}\text{Co}_{0.1}^{3+}\text{Al}_{1.51}^{3+}]$	8.110
1	1400	1	$\text{Co}_{1.39}\text{Al}_{1.61}\text{O}_4$	$(\text{Co}_{0.89}^{2+}\text{Al}_{0.11}^{3+})$	$[\text{Co}_{0.39}^{2+}\text{Co}_{0.11}^{3+}\text{Al}_{1.50}^{3+}]$	8.111
2	1400	1	$\text{CoAl}_2\text{O}_4$	$(\text{Co}_{0.94}^{2+}\text{Al}_{0.06}^{3+})$	$[\text{Co}_{0.06}^{2+}\text{Al}_{1.94}^{3+}]$	8.107

**Table 4.** Structural parameters  $\text{CoAl}_2\text{O}_4$  pigment powders after heat treatment at different temperatures and times.

Sample	Temperature (°C)	Time (h)	Space Group	a (Å)	$\alpha$ (°)	V (Å <sup>3</sup> )	Z	Density
1	1200	1	<i>Fd-3m</i>	8.096	90	533.39	8	4.4053
2	1200	1	<i>Fd-3m</i>	8.104	90	532.37	8	4.4138
1	1200	3	<i>Fd-3m</i>	8.11	90	532.67	8	4.4113
1	1400	1	<i>Fd-3m</i>	8.111	90	533.58	8	4.4037
2	1400	1	<i>Fd-3m</i>	8.107	90	533.18	8	4.5219

Combined with Table 2, heating sample 1 at 1200 °C for 3 h and 1400 °C for 1 h presents a similar phase. At a low temperature, sample 1, nevertheless, obtains a thinner crystallite size, larger crystalline interfaces, and more curved grain boundaries which are unfavorable for crack propagation and development, resulting in better strength and toughness [37,38]. And, increasing the ratio of aluminum can encourage the cation transfer to the normal position in the crystallite to obtain high-quality cobalt blue pigments. Some researchers also demonstrate that the Co/Al ratio should not exceed 0.3 to obtain pure  $\text{CoAl}_2\text{O}_4$  [39]. Gaudon et al. report the same results and explain that the excessive  $\text{Al}^{3+}$  ratio prevents the occurrence of Co ions in octahedral sites due to its higher octahedral site preference energy [23].

Cation distribution is significant to the coloration of cobalt blue and many other kinds of pigments. From our research, controlling the heat treatment and doping of excessive ions in the formula prove effective. To fabricate other relational colors, some cations also have effects on the coloration, such as  $\text{Ni}^{2+}$  and  $\text{Mg}^{2+}$ . They can substitute the  $\text{Co}^{2+}$  in tetrahedral sites and endow the crystallite with a cyan hue [23]. Hence, cation substitution should be researched in the future to prepare various pigments, and cation distribution may be helpful to control and predict the coloration of pigments. Alongside the factors mentioned above, cation substitution should also be considered in the preparation of the solid solution, not only for the color, but also for other properties like magnetic and catalytic performance.

### 2.3. Color Analysis

The selected colorimetry analysis system is CIE-L\*a\*b\* value, and the test result is shown in Table 5. L\* represents the brightness, with a value from 0 to 100; a\* stands for the

component from green to red, with a value from  $-128$  to  $127$ ;  $b^*$  stands for the component from blue to yellow, with a value from  $-128$  to  $127$  [40].

**Table 5.** CIE- $L^*a^*b^*$  colorimetric analysis of  $\text{CoAl}_2\text{O}_4$  pigment powders after heat treatment at different temperatures and times.

Sample	Temperature ( $^{\circ}\text{C}$ )	Time (h)	$L^*$	$a^*$	$b^*$	Color
1	500	1	22.52	$-0.53$	$-11.24$	
1	800	1	14.54	$-2.82$	$-9.44$	
1	1200	1	27.70	$-4.15$	$-27.17$	
2	1200	1	24.60	$-3.74$	$-27.83$	
1	1200	3	27.87	$-3.68$	$-30.80$	
1	1400	1	27.82	$-1.85$	$-31.18$	
2	1400	1	26.41	$7.31$	$-40.54$	

The colorimetric analysis of the samples after heat treatment at different temperatures and time with different ratios are presented. The color of the samples heated at  $500$  and  $800$   $^{\circ}\text{C}$  appears close to black, owing to the  $\text{Co}_3\text{O}_4$  acting as the main phase. Starting from  $1200$   $^{\circ}\text{C}$ , the coloration of samples turns from black to blue, which corresponds to the formation of  $\text{CoAl}_2\text{O}_4$ . This is consistent with XRD patterns in Figure 2. Samples heated at  $1200$   $^{\circ}\text{C}$  for 3 h and  $1400$   $^{\circ}\text{C}$  for 1 h present analogous  $L^*a^*b^*$  values, which can confirm the results of XRD refinement data, i.e., the similar phases of the two samples. The increase in the aluminum ratio proves effective in color because the value  $b^*$  shifts obviously toward blue, which is also in agreement with the report by Gaudon [41]. Throughout all colorimetric values of rising temperature, high temperature and an appropriate ratio provide the best conditions for the formation of  $\text{CoAl}_2\text{O}_4$ .

In essence, the cation distribution should combine with the color. Cobalt, the color element in the spinel, decides on the coloration depending on the valence and site. The distributions of  $\text{Co}^{2+}$  and  $\text{Co}^{3+}$  in tetrahedral or octahedral sites do not have an obvious connection with the  $L^*$  value. In another word, the cation distribution in the cobalt spinel could have nothing to do with the brightness. The value of  $a^*$  has a little bit of connection with the position of  $\text{Co}^{3+}$ , but this little influence is not specific to the naked eye in our samples. The degree of blue is mainly related to the  $b^*$  value. It proposed that if too many  $\text{Co}^{2+}$  occupy the tetrahedral sites, the  $b^*$  value can be smaller.

Diffuse absorbance spectra are an auxiliary approach to the colorimetry analysis of spectroscopic data, and also the variation in the cobalt ions. Figure 7 presents the UV–vis absorption spectra of cobalt blue pigments with diverse formulas, heat temperatures, and heat times. All the spectra show the intensive absorption of visible light in the range of  $500$ – $700$  nm, especially for the ones heated with high temperatures, which corresponds to the blue color region. Moreover, the absorptions at about  $380$  and  $590$  nm represent  $\text{Co}^{3+}$  in octahedral sites and  $\text{Co}^{2+}$  in tetrahedral sites, respectively [42]. This is also characterized as a  $\text{Co}_3\text{O}_4$  cluster due to two board bands at around  $380$  and  $700$  nm for the samples sintered at  $500$   $^{\circ}\text{C}$  [43,44]. As the temperature increases, these absorptions turn out to be weak. The maximal absorptions at near  $540$ ,  $590$ , and  $640$  nm turn to become clear with the heat temperature increase, which indicates the formation of  $\text{CoAl}_2\text{O}_4$ . Additionally, the decline in absorption at about  $380$  nm shows the decrease in  $\text{Co}^{3+}$  in octahedral sites, resulting in a reduction in the green shade.

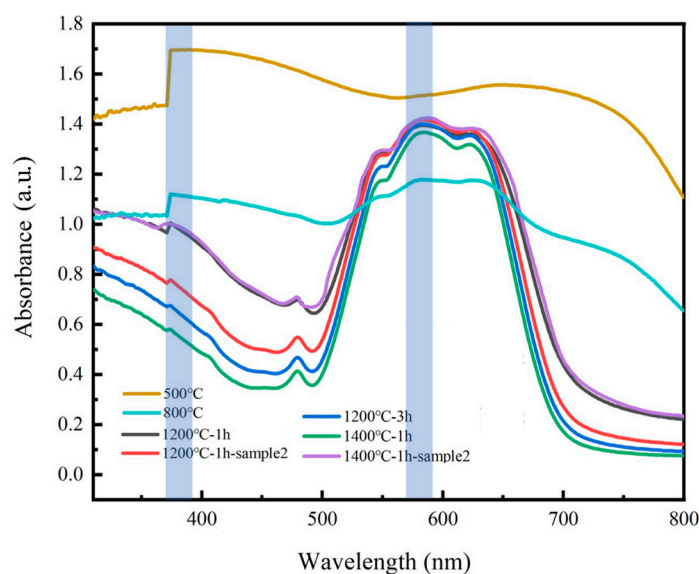


**Figure 7.** UV-vis absorbance spectra of  $\text{CoAl}_2\text{O}_4$  pigment powders after heat treatment at different temperatures and times.

### 3. Experimental

#### 3.1. Synthesis Process

Figure 8 illustrates the fabrication process of samples in this study. With a molar ratio of 1:2, cobalt acetate ( $\text{C}_4\text{H}_6\text{CoO}_4 \cdot 4\text{H}_2\text{O}$ , Aladdin Corp., Shanghai, China) and aluminum nitrate ( $\text{Al}(\text{NO}_3)_3 \cdot 9\text{H}_2\text{O}$ , Aladdin Corp., Shanghai, China) were dissolved separately in water, and then they were mixed together. Under magnetic stirring at 500 rpm,  $\text{NH}_3 \cdot \text{H}_2\text{O}$  was added dropwise to reach a pH of about 9; however, the quantity of the  $\text{NH}_3 \cdot \text{H}_2\text{O}$  can be a little more than needed. Then, we continued to stir for 2.5 h to mix them homogeneously. The precursors were separated with a centrifugal machine, and then the precipitates were washed with absolute ethanol to neutralize them in order to obtain cobalt and aluminum hydroxide alcohol mixtures. Then, the jelly-like gel was subject to heat treatment and sintering at 250 °C, 500 °C, 800 °C, 1200 °C, and 1400 °C for 1 h each. The fabrication process was repeated with an excessive proportion of aluminum (ratio of cobalt and aluminum is 1:3) to obtain another batch of precursors. Then, they were heated under different temperatures.

#### 3.2. Characterization

The as-prepared powders were characterized by thermo gravimetry–differential scanning calorimetry (TG–DSC, STA 449 F5, Netzsch, Selb, Germany), X-ray diffraction (XRD, D/MAX2500VL/PC, Rigaku, Tokyo, Japan), energy dispersive spectroscopy (EDS, Hitachi S-800, Hitachi, Tokyo, Japan), and a spectrodensitometer (FD-5, Konica Minolta, Tokyo, Japan). XRD measurements were carried out with a X-celerator detector, using  $\text{Cu}(\text{K}\alpha_1/\text{K}\alpha_2)$  radiation. Diffractograms were analyzed via the Rietveld refinement method with a software program named *Jade 6.0*. Debye Scherrer's Equation (1) was used with the widths of the peak to evaluate crystallite sizes [30].

$$D = \frac{K\gamma}{B\cos\theta} \quad (1)$$

where  $D$  is the average thickness of the crystal grain perpendicular of the crystal plane,  $K$  is the Scherrer constant,  $\gamma$  is the X-ray wavelength (generally 1.54056 Å),  $B$  is the half-height width or integral width of the measured sample diffraction peak, and  $\theta$  is the Bragg angle in degrees.

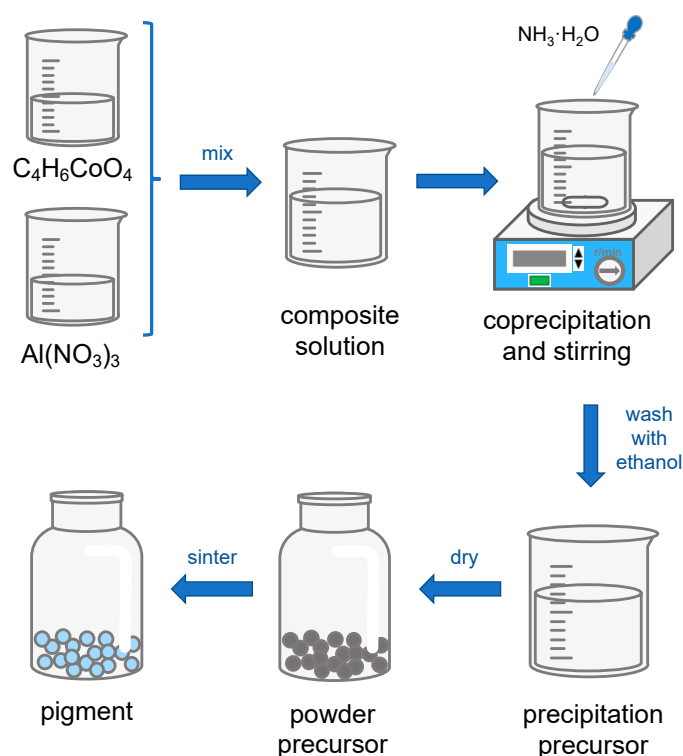


Figure 8. Synthesis process of cobalt blue pigments.

#### 4. Conclusions

In this paper, we have prepared cobalt blue pigments using the coprecipitation method, where the heating temperature, time, and ratio of cobalt and aluminum have been set as the variables. The as-fabricated samples were investigated using TG–DSC, XRD, EDS, and colorimetry analysis. Then, Rietveld refinement was implemented to obtain the crystallite data, including the crystallite size, cation distribution, chemical formula, and lattice parameter.

The color change is related to macro and micro perspectives. On the one hand, the color is corresponding to the composition. When the heating temperature is under  $800\text{ }^\circ\text{C}$ ,  $Co^{3+}$  exists in the octahedral site of spinel, so the color appears to lack a blue hue. On the other hand, when the sintering temperature comes to  $1200\text{ }^\circ\text{C}$  or more, the phase of  $CoAl_2O_4$  will become purer.  $Co^{2+}$  in the tetrahedral sites can make the  $b^*$  value small, which indicates that the color of the samples tends to be blue. The cation distribution could be controlled by the heat treatment and stoichiometric ratio. High heat-treatment temperature, long heat-treatment time, and excessive aluminum content play important roles in controlling the cation positions for pure cobalt blue pigments. The results have the potential for energy saving and color prediction in the fabrication process of cobalt blue and other related Co-based pigments.

**Author Contributions:** Methodology, W.Z. (Weiran Zhang), Z.L. and G.W.; software, W.Z. (Weiran Zhang), Z.L., W.W. and H.Z.; resources, G.W.; writing—original draft preparation, W.Z. (Weiran Zhang); writing—review and editing, W.Z. (Weiran Zhang), W.W., H.Z. and H.J.; visualization, Q.X.; supervision, H.J., W.Z. (Weili Zhang) and R.W.; project administration, H.J., W.Z. (Weili Zhang) and R.W.; funding acquisition, H.J. and Q.X. All authors have read and agreed to the published version of the manuscript.

**Funding:** The authors gratefully acknowledge the support from the Projects of Hunan Provincial Department of Education (21C0435), the Science and Technology Innovation Program of Hunan Province (2021RC4065), and the Key Research and Development Program of Hunan Province (2022GK2037).

**Data Availability Statement:** The authors confirm that the data supporting the findings of this study are available within the article.

**Conflicts of Interest:** The authors declare that they have no known competing financial interest or personal relationship that could have appeared to influence the work reported in this paper.

## References

1. Bernardi, M.; Feitosa, C.; Paskocimas, C.; Longo, E.; Paiva-Santos, C. Development of metal oxide nanoparticles by soft chemical method. *Ceram. Int.* **2009**, *35*, 463–466. [[CrossRef](#)]
2. Akdemir, S.; Ozel, E.; Suvaci, E. Solubility of blue  $\text{CoAl}_2\text{O}_4$  ceramic pigments in water and diethylene glycol media. *Ceram. Int.* **2011**, *37*, 863–870. [[CrossRef](#)]
3. Merino, M.C.G.; Estrella, A.L.; Rodriguez, M.E.; Acuña, L.; Lassa, M.S.; Lascalea, G.E.; Vázquez, P. Combustion Syntheses of  $\text{CoAl}_2\text{O}_4$  Powders Using Different Fuels. *Procedia Mater. Sci.* **2015**, *8*, 519–525. [[CrossRef](#)]
4. Wu, T.; Sun, S.; Song, J.; Xi, S.; Du, Y.; Chen, B.; Sasangka, W.A.; Liao, H.; Gan, C.L.; Scherer, G.G.; et al. Iron-facilitated dynamic active-site generation on spinel  $\text{CoAl}_2\text{O}_4$  with self-termination of surface reconstruction for water oxidation. *Nat. Catal.* **2019**, *2*, 763–772. [[CrossRef](#)]
5. Angeletti, C.; Pepe, F.; Porta, P. Structure and catalytic activity of  $\text{Co}_x\text{Mg}_{1-x}\text{Al}_2\text{O}_4$  spinel solid solutions. Part 1.—Cation distribution of  $\text{Co}^{2+}$  ions. *J. Chem. Soc. Faraday Trans. 1 Phys. Chem. Condens. Phases* **1977**, *73*, 1972–1982. [[CrossRef](#)]
6. Llusar, M.; Forés, A.; Badenes, J.; Calbo, J.; Tena, M.; Monrós, G. Colour analysis of some cobalt-based blue pigments. *J. Eur. Ceram. Soc.* **2001**, *21*, 1121–1130. [[CrossRef](#)]
7. Monari, G.; Manfredini, T. Coloring Effects of Synthetic Inorganic Cobalt Pigments in Fast-Fired Porcelainized Tiles. In *A Collection of Papers Presented at the 97th Annual Meeting and the 1995 Fall Meetings of the Materials & Equipment/Whitewares: Ceramic Engineering and Science Proceedings*; Wachtman, J.B., Jr., Ed.; The American Ceramic Society: Columbus, OH, USA, 1996; Volume 17, pp. 167–172. [[CrossRef](#)]
8. Tatarchuk, T.; Bououdina, M.; Paliychuk, N.; Yaremiy, I.; Moklyak, V. Structural characterization and antistructure modeling of cobalt-substituted zinc ferrites. *J. Alloys Compd.* **2017**, *694*, 777–791. [[CrossRef](#)]
9. Agilandeswari, K.; Kumar, A.R. Synthesis, characterisation, optical and luminescence properties of  $\text{CoAl}_2\text{O}_4$ . *AIP Conf. Proc.* **2015**, *1665*, 120022. [[CrossRef](#)]
10. Hudson, K.; Winbow, H.; Cowley, J. Colors for Ceramic Bodies. In *A Collection of Papers Presented at the 97th Annual Meeting and the 1995 Fall Meetings of the Materials & Equipment/Whitewares: Ceramic Engineering and Science Proceedings*; Wachtman, J.B., Jr., Ed.; The American Ceramic Society: Columbus, OH, USA, 1996; Volume 17, pp. 102–110. [[CrossRef](#)]
11. Li, W.; Li, J.; Guo, J. Synthesis and characterization of nanocrystalline  $\text{CoAl}_2\text{O}_4$  spinel powder by low temperature combustion. *J. Eur. Ceram. Soc.* **2003**, *23*, 2289–2295. [[CrossRef](#)]
12. Cho, W.-S.; Kakihana, M. Crystallization of ceramic pigment  $\text{CoAl}_2\text{O}_4$  nanocrystals from Co–Al metal organic precursor. *J. Alloys Compd.* **1999**, *287*, 87–90. [[CrossRef](#)]
13. Pozas, R.; Orera, V.; Ocaña, M. Hydrothermal synthesis of Co-doped willemite powders with controlled particle size and shape. *J. Eur. Ceram. Soc.* **2005**, *25*, 3165–3172. [[CrossRef](#)]
14. Hu, Z.; Xue, M.; Zhang, Q.; Sheng, Q.; Liu, Y. Nanocolorants: A novel class of colorants, the preparation and performance characterization. *Dye. Pigment.* **2008**, *76*, 173–178. [[CrossRef](#)]
15. Zhang, W.; Li, J.; Zhong, F.; Wu, G.; Jiang, H.; Zhang, W.; Liu, Q. Preparation and characterization of supercritical fluid-fried ( $\text{CoAl}_2\text{O}_4$ ) cobalt blue nano-pigment. *J. Asian Ceram. Soc.* **2021**, *10*, 33–39. [[CrossRef](#)]
16. Yuan, S.; Yuanlin, Z.; Yufei, T.; Yangfeng, J. Fabrication and Coloration Mechanism of  $\text{CoAl}_2\text{O}_4$  Ceramic Pigment by Coprecipitation Method. *J. Synth. Cryst.* **2017**, *46*, 79–84.
17. Zhang, A.; Mu, B.; Luo, Z.; Wang, A. Bright blue halloysite/ $\text{CoAl}_2\text{O}_4$  hybrid pigments: Preparation, characterization and application in water-based painting. *Dye. Pigment.* **2017**, *139*, 473–481. [[CrossRef](#)]
18. Ahmed, I.; Shama, S.; Moustafa, M.; Dessouki, H.; Ali, A. Synthesis and spectral characterization of  $\text{Co}_x\text{Mg}_{1-x}\text{Al}_2\text{O}_4$  as new nano-coloring agent of ceramic pigment. *Spectrochim. Acta Part A Mol. Biomol. Spectrosc.* **2009**, *74*, 665–672. [[CrossRef](#)] [[PubMed](#)]
19. Xin, L.; Jiak, L.; Kai, C. Preparation of Spinel Type  $\text{Zn}_x\text{Co}_{1-x}\text{Al}_2\text{O}_4$  Ultrafine Ceramic Pigment by Solution Combustion Method. *J. Synth. Cryst.* **2014**, *43*, 2086–2090.
20. Gilibert, J.; Palacios, Sanz, V.; Mestre, S. Characteristics reproducibility of  $(\text{Fe}, \text{Co})(\text{Cr}, \text{Al})_2\text{O}_4$  pigments obtained by solution combustion synthesis. *Ceram. Int.* **2016**, *42*, 12880–12887. [[CrossRef](#)]
21. Chemlal, S.; Larbot, A.; Persin, M.; Sarrazin, J.; Sghyar, M.; Rafiq, M. Cobalt spinel  $\text{CoAl}_2\text{O}_4$  via sol-gel process: Elaboration and surface properties. *Mater. Res. Bull.* **2000**, *35*, 2515–2523. [[CrossRef](#)]
22. Valenzuela, M.; Bosch, P.; Aguilar-Rios, G.; Montoya, A.; Schifter, I. Comparison Between Sol-Gel, Coprecipitation and Wet Mixing Synthesis of  $\text{ZnAl}_2\text{O}_4$ . *J. Sol-Gel Sci. Technol.* **1997**, *8*, 107–110. [[CrossRef](#)]
23. Gaudon, M.; Robertson, L.; Lataste, E.; Duttine, M.; Ménétrier, M.; Demourgues, A. Cobalt and nickel aluminate spinels: Blue and cyan pigments. *Ceram. Int.* **2014**, *40*, 5201–5207. [[CrossRef](#)]
24. Fernández-Osorio, A.; Pineda-Villanueva, E.; Chávez-Fernández, J. Synthesis of nanosized  $(\text{Zn}_{1-x}\text{Co}_x)\text{Al}_2\text{O}_4$  spinels: New pink ceramic pigments. *Mater. Res. Bull.* **2012**, *47*, 445–452. [[CrossRef](#)]

25. Tsurumi, T.; Hirayama, H.; Vacha, M.; Taniyama, T. *Nanoscale Physics for Materials Science*; CRC Press: Boca Raton, FL, USA, 2009. [[CrossRef](#)]
26. Zawadzki, M.; Wrzyszczyk, J. Hydrothermal synthesis of nanoporous zinc aluminate with high surface area. *Mater. Res. Bull.* **2000**, *35*, 109–114. [[CrossRef](#)]
27. Zhang, A.; Mu, B.; Hui, A.; Wang, A. A facile approach to fabricate bright blue heat-resisting paint with self-cleaning ability based on  $\text{CoAl}_2\text{O}_4$ /kaolin hybrid pigment. *Appl. Clay Sci.* **2018**, *160*, 153–161. [[CrossRef](#)]
28. Angeletti, C.; Pepe, F.; Porta, P. Structure and catalytic activity of  $\text{Co}_x\text{Mg}_{1-x}\text{Al}_2\text{O}_4$  spinel solid solutions. Part 2.—Decomposition of  $\text{N}_2\text{O}$ . *J. Chem. Soc. Faraday Trans. 1 Phys. Chem. Condens. Phases* **1978**, *74*, 1595–1603. [[CrossRef](#)]
29. Zayat, M.; Levy, D. Blue  $\text{CoAl}_2\text{O}_4$  Particles Prepared by the Sol–Gel and Citrate–Gel Methods. *Chem. Mater.* **2000**, *12*, 2763–2769. [[CrossRef](#)]
30. Holzwarth, U.; Gibson, N. The Scherrer equation versus the ‘Debye-Scherrer equation’. *Nat. Nanotechnol.* **2011**, *6*, 534. [[CrossRef](#)] [[PubMed](#)]
31. Mindru, I.; Marinescu, G.; Gingasu, D.; Patron, L.; Ghica, C.; Giurginca, M. Blue  $\text{CoAl}_2\text{O}_4$  spinel via complexation method. *Mater. Chem. Phys.* **2010**, *122*, 491–497. [[CrossRef](#)]
32. Zhang, A.; Wang, N.; Mu, B.; Li, H.; Wang, A. Amino-acid-assisted preparation of  $\text{CoAl}_2\text{O}_4$ /kaolin hybrid pigments. *Appl. Clay Sci.* **2020**, *191*, 105611. [[CrossRef](#)]
33. Peng, X.; Cheng, J.; Yuan, J.; Jin, N.; Kang, J.; Hou, Y.; Zhang, Q. Environmental blue  $\text{CoAl}_2\text{O}_4$  pigment co-doped by  $\text{Zn}^{2+}$  and  $\text{Mg}^{2+}$ : Synthesis, structure and optical properties. *Adv. Appl. Ceram.* **2017**, *117*, 303–311. [[CrossRef](#)]
34. Lilova, K.I.; Navrotsky, A.; Melot, B.C.; Seshadri, R. Thermodynamics of  $\text{CoAl}_2\text{O}_4$ – $\text{CoGa}_2\text{O}_4$  solid solutions. *J. Solid State Chem.* **2010**, *183*, 1266–1271. [[CrossRef](#)]
35. Wong-Ng, W.; McMurdie, H.; Hubbard, C.; Mighell, A. JCPDS-ICDD Research Associateship (cooperative program with NBS/NIST). *J. Res. Natl. Inst. Stand. Technol.* **2001**, *106*, 1013–1028. [[CrossRef](#)]
36. Visinescu, D.; Paraschiv, C.; Ianculescu, A.; Jurca, B.; Vasile, B.; Carp, O. The environmentally benign synthesis of nanosized  $\text{Co}_x\text{Zn}_{1-x}\text{Al}_2\text{O}_4$  blue pigments. *Dye. Pigment.* **2010**, *87*, 125–131. [[CrossRef](#)]
37. Chen, Z.-Z.; Shi, E.-W.; Li, W.-J.; Zheng, Y.-Q.; Zhuang, J.-Y.; Xiao, B.; Tang, L.-A. Preparation of nanosized cobalt aluminate powders by a hydrothermal method. *Mater. Sci. Eng. B* **2004**, *107*, 217–223. [[CrossRef](#)]
38. Yu, F.; Yang, J.; Ma, J.; Du, J.; Zhou, Y. Preparation of nanosized  $\text{CoAl}_2\text{O}_4$  powders by sol–gel and sol–gel-hydrothermal methods. *J. Alloys Compd.* **2009**, *468*, 443–446. [[CrossRef](#)]
39. Štangar, U.L.; Orel, B.; Krajnc, M. Preparation and Spectroscopic Characterization of Blue  $\text{CoAl}_2\text{O}_4$  Coatings. *J. Sol-Gel Sci. Technol.* **2003**, *26*, 771–775. [[CrossRef](#)]
40. Luo, M.R.; Cui, G.; Rigg, B. The development of the CIE 2000 colour-difference formula: CIEDE2000. *Color Res. Appl.* **2001**, *26*, 340–350. [[CrossRef](#)]
41. Gaudon, M.; Apheceixborde, A.; Ménétrier, M.; Le Nestour, A.; Demourgues, A. Synthesis Temperature Effect on the Structural Features and Optical Absorption of  $\text{Zn}_{1-x}\text{Co}_x\text{Al}_2\text{O}_4$  Oxides. *Inorg. Chem.* **2009**, *48*, 9085–9091. [[CrossRef](#)]
42. Vandewater, L.; Bezemer, G.L.; Bergwerff, J.A.; Versluijsghelder, M.; Weckhuysen, B.M.; Dejong, K. Spatially resolved UV–vis microspectroscopy on the preparation of alumina-supported Co Fischer–Tropsch catalysts: Linking activity to Co distribution and speciation. *J. Catal.* **2006**, *242*, 287–298. [[CrossRef](#)]
43. Liotta, L.; Pantaleo, G.; Macaluso, A.; Di Carlo, G.; Deganello, G. CoOx catalysts supported on alumina and alumina-baria: Influence of the support on the cobalt species and their activity in NO reduction by  $\text{C}_3\text{H}_6$  in lean conditions. *Appl. Catal. A Gen.* **2003**, *245*, 167–177. [[CrossRef](#)]
44. Dhas, C.R.; Venkatesh, R.; Jothivenkatachalam, K.; Nithya, A.; Benjamin, B.S.; Raj, A.M.E.; Jeyadheepan, K.; Sanjeeviraja, C. Visible light driven photocatalytic degradation of Rhodamine B and Direct Red using cobalt oxide nanoparticles. *Ceram. Int.* **2015**, *41*, 9301–9313. [[CrossRef](#)]

**Disclaimer/Publisher’s Note:** The statements, opinions and data contained in all publications are solely those of the individual author(s) and contributor(s) and not of MDPI and/or the editor(s). MDPI and/or the editor(s) disclaim responsibility for any injury to people or property resulting from any ideas, methods, instructions or products referred to in the content.